ACS OMEGA

http://pubs.acs.org/journal/acsodf

Article

Electric-Field-Effect Spin Switching with an Enhanced Number of Highly Polarized Electron and Photon Spins Using p-Doped Semiconductor Quantum Dots

Soyoung Park, Hang Chen, Satoshi Hiura, Junichi Takayama, Kazuhisa Sueoka, and Akihiro Murayama*

Cite This: *ACS Omega* 2021, 6, 8561−8569

Read Online

ACCESS | Metrics & More | Article Recommendations

ABSTRACT: Electric-field-effect spin switching with an enhanced number of highly polarized electron and photon spins has been demonstrated using p-doped semiconductor quantum dots (QDs). Remote p-doping in InGaAs QDs tunnel-coupled with an InGaAs quantum well (QW) significantly increased the circularly polarized, thus electron-spin-polarized, photoluminescence intensity, depending on the electric-field-induced electron spin injection from the QW as a spin reservoir into the QDs. The spin polarity and polarization degree during this spin injection can be controlled by the direction and the strength of the electric field, where the spin direction can be reversed by excess electron spin injection into the QDs via spin scattering at the QD excited states. We found that the maximum degrees of both parallel and antiparallel spin polarization to the initial spin direction in the QW can be enhanced by p-doping. The doped holes without spin polarization can effectively contribute to this electric-field-effect spin switching after the initial electron spin injection selectively removes the parallel hole spins. The optimized p-doping induces fast spin reversals at the QD excited states with a moderate electric-field application, resulting in an efficient electric-field-driven antiparallel spin injection into the QD ground state. Further excess hole doping prevents this efficient spin reversal due to multiple electron−hole spin scattering, in addition to a spin-state filling effect at the QD excited states, during the spin injection from the QW into the QDs.

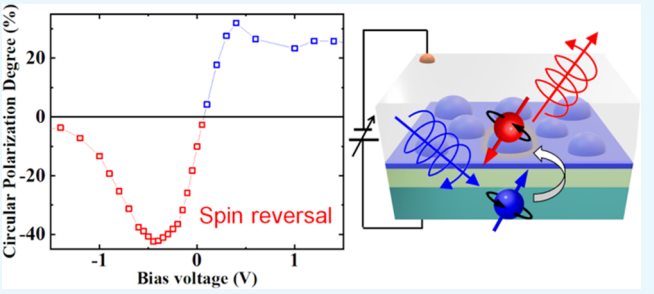

1. INTRODUCTION

Spin polarizations of an electron and photon/light are essential properties of these information carriers, where the photon spin is known as its circular polarization. These spin characteristics can be directly converted into each other by photoelectric conversion in III−V compound semiconductor optically active layers, taking the optical selection rule into consideration.[1,2] This photoelectric conversion maintaining the electron and photon spin polarizations has been extensively studied due to its potential applications in spin-functional optical devices, in addition to fundamental interests. The electron spin polarization can be conserved without consuming electrical power in ferromagnetic metallic materials, such as Fe and Co, and these alloys are one of the most promising solid-state memories with reliable read/write operations.[3−6] On the other hand, III−V compound semiconductors, such as GaAs, and the related compounds are widely known as the most useful materials for practical optical devices, such as light-emitting diodes and lasers for optical communication. Furthermore, self-assembled quantum dots (QDs) of III−V compound semiconductors, such as InGaAs and InAs with three-dimensional (3D) quantum confinements, have been studied to realize highly efficient photoelectric conversion owing to the discrete density of the electron states and the high oscillator strength.[7−12] A QD-based optically active laser has already been established, in which temperature-insensitive emitting performances were demonstrated owing to strong suppression of thermal electron distribution at a limited density of the states, which was caused by the abovementioned strong quantum confinement.[13,14] This strong confinement of the QD is also very attractive as it offers an additional benefit of strong suppression of electron spin relaxation.[15−19] The spin relaxation in the QDs can be suppressed, resulting in the spin-relaxation time constants of a couple of nanoseconds at low temperatures during photoelectric conversion with emission decay times of less than 1 ns. This means that one can transfer the electron spin polarization in the ferromagnetic material to the circular polarization of the emission light (light spin information), using the semiconductor QD-based active layer,

Received: January 21, 2021
Accepted: March 3, 2021
Published: March 15, 2021

ACS Publications

© 2021 The Authors. Published by American Chemical Society

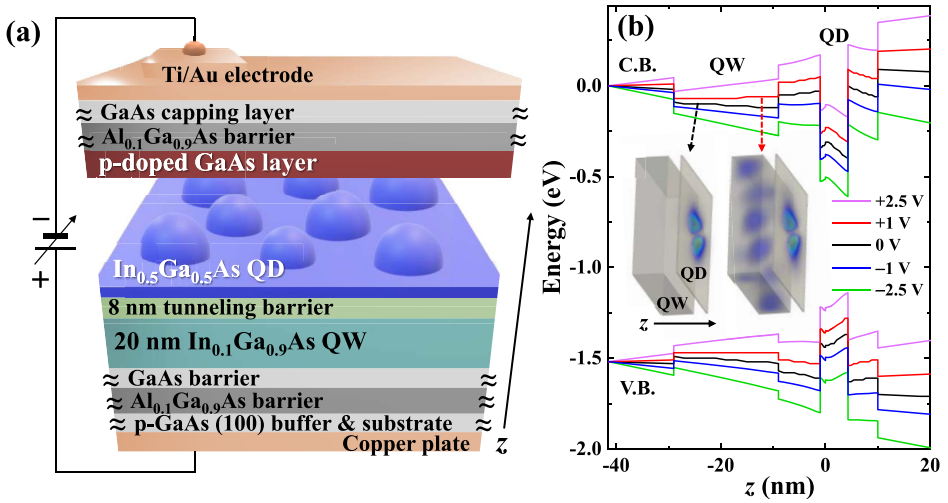

Figure 1. (a) Schematic cross-sectional drawing of the electric-field-effect optical-spin device with a QW/QD-coupled active layer, used in this study. (b) Potentials of the QW/QD-coupled conduction and valence bands along the growth direction (z-axis), where $z = 0$ is set at the bottom of the QD, calculated as a function of the applied voltage between −2.5 and +2.5 V. The conduction band potentials are plotted to be 0 eV at $z = -42$ nm. The insets show the 3D-calculated electron wavefunctions at the first excited state of the QD coupled with the QW with applied voltages of 0 V (left) and +1 V (right).

if an efficient spin injection from the former ferromagnetic spin injector into the latter QD spin emitter is established. This attempt has been demonstrated by fabricating a spin-polarized light-emitting diode (spin LED) using a self-assembled QD ensemble layer with a di-electrode device structure.[20−23]

The next attempt is to develop electric-field effects on spin polarity and its polarization degree, where the electric-field functionality is an essential prerequisite for electronics. For this purpose, semiconductor QDs are also useful. Electric-field reversal of electron spin polarity has recently been demonstrated using a spin injection process from a 2D quantum well (QW) into 0D QDs.[24] The number of electrons injected into the QD can be controlled by electric-field modification of the coupled potential between the QW and QD. Excess electrons at the excited states (ESs) in the QD, which can be transiently maintained by the existence of the ground state (GS) residual electrons through Pauli's exclusion rule, can be scattered by holes. As a result, the electron spin direction can flip at these ESs and then relax to the GS.[24,25] The presence of excess electrons in the QD is essential for this spin reversal mechanism.[24−31] The highly limited space of the QD can cause the spin reversal via electron−hole scattering more efficiently. The spin injection from the QW as a spin reservoir is also important to precisely control the number of injected electrons through the electric-field direction and strength. Moreover, it has been reported that p-doping in the QD can vary the electric-field conditions necessary to reverse the spin polarity.[24] The resonant electron spin tunneling responsible for the above spin injection through this heterodimensional-coupled potential between the 2D QW and 0D QD has also been clarified.[24,32]

This unique QW/QD-coupled optical spin-active layer can offer a new platform for electric-field-effect spin-functional optical devices. The electric-field manipulation of an electron and its spin state is an important function of semiconductor materials, and the resultant spin information can be smoothly transferred by light after spin manipulation. In contrast, generally speaking, the spin direction is strongly fixed in ferromagnetic metallic materials such as Fe and Co in addition to fact that the electric field cannot work in those metals. New methods have been proposed to control the spin and magnetization of metallic materials using spin transfer or spin−orbit torque.[33−36] On the other hand, the above electric-field control of spin using a semiconductor QW/QD-coupled nanosystem is attractive and needs to be studied to enhance the device performance. One important subject is to examine the effect of p-doping. The other one is to elucidate the time-dependent spin dynamics including the spin-flip process at the QD-ES just after spin injection from the QW, which is responsible for this electric-field-induced spin reversal. A systematic study has been conducted to investigate these important subjects: p-doping effects on the electric-field control of spin manipulation as well as on the spin-flip dynamics at the ES. As a result, the optimized p-doping concentration was found to enhance the electric-field effects significantly in terms of both emission intensity and spin operation efficiency. The spin dynamics at the ES clarify efficient spin scattering at this optimized p-doping condition.

2. EXPERIMENTAL PROCEDURES

The electric-field-effect optical spin devices used in this study were grown on a p-doped (100) GaAs substrate with an undoped 200-nm-thick GaAs buffer layer via molecular beam epitaxy, basically in a similar manner to previous reports.[24,32] Therefore, important points for this study are briefly described as follows: a single $In_{0.5}Ga_{0.5}As$ QD layer with a sheet density of 1.9×10^{10} cm^{-2} was coupled with a bottom 20-nm-thick $In_{0.1}Ga_{0.9}As$ QW by an 8 nm-thick GaAs tunneling barrier. The 10-nm-thick p-doped GaAs capping layers with different Be concentrations were directly stacked on the QD layer. The Be concentration was varied between 1×10^{17} cm^{-3} (corresponding to 5 holes/QD if all holes are injected) and 3×10^{17} cm^{-3} (15 holes/QD), respectively. An undoped sample (0 hole/QD) was also prepared at identical growth conditions as a reference sample. This QW/QD-coupled nanostructure was sandwiched between $Al_{0.1}Ga_{0.9}As$ barriers to prevent carrier injection from a top Ti/Au electrode deposited on the semiconductor surface for an electric-field application. The

https://dx.doi.org/10.1021/acsomega.1c00377
ACS Omega 2021, 6, 8561−8569

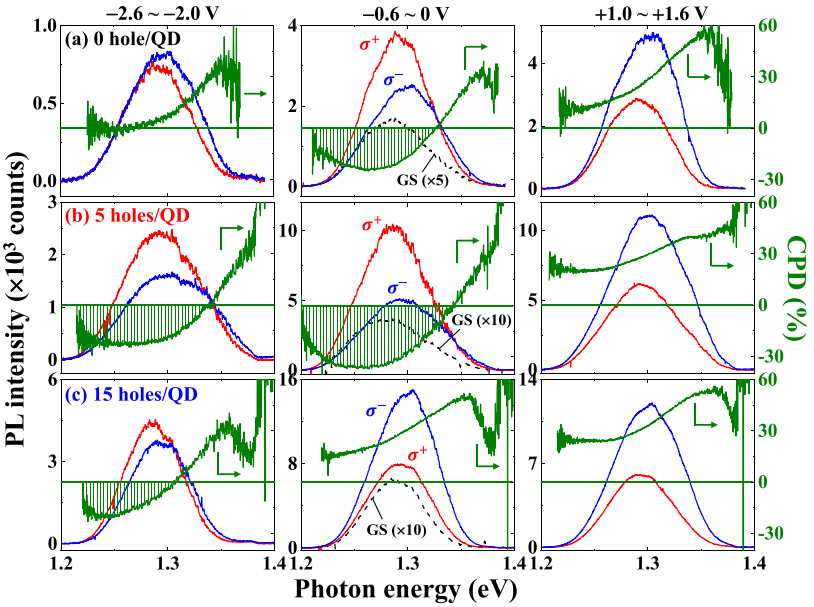

Figure 2. Circularly polarized QD-PL spectra (red solid line: σ^+ as antiparallel polarization to the initial one in the QW; blue solid line: σ^- as parallel polarization to the QW one) and the corresponding CPD values as a function of photon energy (green solid line) with a typical negative (averaged in the range of −2.6 to −2.0 V), near-zero (−0.6 to 0 V), and positive (+1.0 to +1.6 V) biases and an excitation power of 160 μW, for the (a) 0 hole/QD, (b) 5 holes/QD, and (c) 15 holes/QD samples, respectively. A black broken line indicates the PL intensity in the excitation case of 10 μW, where the spectral component shows GS emissions of the QD ensemble. The energy-dependent CPD components indicating negative values, i.e., spin-flip emissions are shown by a green hatched area, where this negative CPD spectral component mainly originates from the GS.

cross-sectional layered structure of this electric-field device is schematically illustrated in Figure 1a.

3D potential calculations of the semiconductor layered structure were performed by varying the electric-field strength.[37] Typical results are shown in Figure 1b, where the 1D potential along the electric-field direction is shown at the center position of a QD. By increasing the electric-field strength with a negative sign, the electron potential (conduction band) in the QD reduces compared to that in the coupled QW, which can promote the injection of spin-polarized electrons via tunneling from the QW into the QDs. The typical coupled electron wavefunctions are shown as insets of Figure 1b.

Optical excitation for spin generation in the QW was performed through a mode-locked Ti:sapphire pulsed laser with a repetition rate of 80 MHz. A temporal width of 200 fs and a combination of the quarter-wave plate with a linear polarizer were used to circularly polarize the laser light, as well as to detect circular polarizations of emissions from the device. To generate spin-polarized carriers in the QW, the photon energy of the laser was tuned to 1.46 eV below the band gap of the GaAs barrier. The excitation power was changed from 10 to 640 μW. The samples were attached to a copper plate on a cold finger of the cryostat and maintained at 4 K. A voltage with a range of −3 to +3 V was applied along the growth direction (z-axis in Figure 1a). Spin-polarized carriers generated in the QW, resulting from the optical selection rule, can be injected via spin-conserving tunneling into the QDs and then detected by circularly polarized photoluminescence (PL) from the QDs. Here, the degree of circular polarization of the PL was defined as CPD = $\{(I_{\sigma-} - I_{\sigma+})/(I_{\sigma-} + I_{\sigma+})\} \times 100$ [%], where $I_{\sigma-}$ and $I_{\sigma+}$ were co- and cross-circularly polarized PL intensities from the QD spin detector after σ^- excitation in the QW spin reservoir. This CPD value directly reflects the *electron spin polarization* P at emissive states in the QD, defined as $P = \{(N_\uparrow - N_\downarrow)/(N_\uparrow + N_\downarrow)\} \times 100$ [%] with the number of parallel and antiparallel electron spins ($N_{\uparrow\downarrow}$) to the initial QW ones, owing to the optical selection rule.[1]

3. RESULTS AND DISCUSSION

Figure 2 shows circularly polarized PL spectra and the corresponding energy-dependent CPD values at 4 K with typical negative (−2.6 to −2.0 V), near-zero (−0.6 to 0 V), and positive (+1.0 to +1.6 V) biases for the (a) 0, (b) 5, and (c) 15 holes/QD samples.

The 0 hole/QD reference sample indicates the negative CPD (antiparallel circular polarization to the initial polarization in the QW, thus spin-flip injection) at 0 V, while the positive CPD (parallel circular polarization, thus normal spin injection) is observed at the other positive and negative biases. The larger positive spin-polarization degrees are observed for the higher energy tail of the PL spectra in Figure 2. This higher energy tail with higher positive CPDs originates from emissions at ESs in the QDs after spin injection from the QW, which is known from a lower-energy QD-GS spectrum obtained with an extremely low excitation condition (a black broken line). At ESs, the higher density of states can suppress state-filling-induced degradation of the spin polarization after the parallel spin injection from the QW.[38,39] As a result, higher CPDs at the ES spectral component can be observed than those at the GS one. The negative CPD region appears only at the GS of the QD ensemble with various shape and size distributions. The appearance of the negative CPD can be attributed to spin-flip scattering at the ES just after the injection of spin-polarized electrons from the QW. The presence of residual electrons with the parallel polarization to the initial QW spin polarization at the QD-GS can induce electron−hole spin scattering at the ES due to the Pauli spin blocking, in which the spin-flipped electron only can relax to

https://dx.doi.org/10.1021/acsomega.1c00377
ACS Omega 2021, 6, 8561−8569

the GS, and then emit the PL with negative CPD.[24,25] In fact, the coupled QW/QD conduction potential tilts slightly toward the QD side at this 0 V, as shown in Figure 1b, while the valence-band potential exhibits an opposite trend. Therefore, electrons initially generated in the QW can be smoothly injected into the QD via tunneling, whereas holes are likely to localize at the QW. This situation means that the number of injected electrons can increase compared to that of holes, and excess electrons can be injected from the QW into the QDs. More precise bias dependence of the carrier and spin dynamics will be discussed later. The appearance of this negative PL-CPD and the bias dependence are significantly affected by p-doping, as shown in Figure 2.

The QD-PL intensity and the corresponding CPD value as a function of bias are plotted in Figure 3, for all three samples.

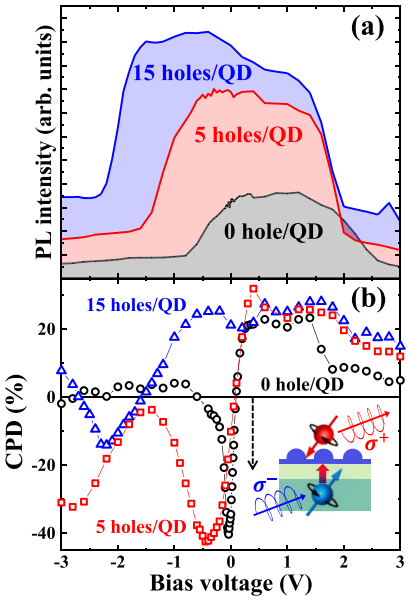

Figure 3. (a) PL intensity and (b) the CPD value at the QD-GS as a function of bias with an excitation power of 160 μW for the 0 hole/QD (a black line in (a) and black open circles in (b)), 5 holes/QD (a red line in (a) and red open squares in (b)), and 15 holes/QD (a blue line in (a) and blue open triangles in (b)) samples. The spin-flip injection process with negative CPD values are schematically shown as an inset in (b).

As can be seen in Figure 3a, the PL intensity of the 0 hole/QD reference sample is markedly lower, while the p-doping can significantly increase the emission intensity. The basic trend of the bias dependence of the PL intensity is identical among those samples; the PL intensity decreases at higher positive as well as negative biases. The former decrease in the PL intensity higher than approximately +1.5 V is attributed to the suppression of electron tunneling from the QW into the QD side, as shown in the potential calculations in Figure 1b. The latter PL decrease originates from the hole localization at the QW side, also as shown in Figure 1b. The starting bias of this PL decrease at the negative bias side is systematically dependent on the p-doping concentration: 0 V for 0 hole/QD, −0.6 V for 5 holes/QD, and −1.7 V for 15 holes/QD samples. This can be understood by the fact that remote p-doping of the QDs from the upper QD capping layer can compensate for hole depletion at negative bias regions, where the valence-band potential of the QD increases and the photogenerated holes cannot be injected from the QW. The PL intensity does not change significantly over a relatively wide bias range, especially for doped samples. The PL intensity can be dominated by the number of minority carriers between an electron and a hole. Therefore, this plateau-like behavior can be attributed to a certain number of minority carriers at the GS. Electron deficiency commonly reduces the PL intensity toward higher positive biases, while hole deficiencies are compensated for by doping to the negative bias side. Moreover, the PL intensity at moderate bias conditions is greatly enhanced by this p-doping; 2.3 times higher in the 5 holes/QD sample and 2.8 times higher in the 15 holes/QD sample than in the undoped reference sample, respectively. This drastic change in the PL intensity can be attributed to an increase in the number of holes in the QDs. Our remote p-doping using direct stacking of the upper capping layer with controlled Be concentrations is highly effective for enhancing the emission efficiency without a significant carrier loss due to the degradation of the QD crystal quality. Meanwhile, this increased number of holes by p-doping can change the occurrence of excess electrons in the QDs. Figure 3b shows the effect of p-doping on the spin injection process, which can be described as follows: a strong negative CPD appears at 0 V in the 0 hole/QD sample, as mentioned above. This characteristic bias (∼0 V) corresponds to the starting bias of the PL intensity reduction, which supports the existence of excess electrons due to the imbalance between the enhanced electron injection and the reduction of hole injection from the QW to the QDs. It should be noted that this bias range promoting the electric-field-induced spin reversal is rather narrow. In contrast, in the 5 holes/QD sample, more negative biases peaking at −0.5 V show a similarly large degree of negative circular polarization. This bias condition also agrees well with the decrease in the starting bias of PL. Therefore, the p-doping shifts the bias condition necessary to induce the spin-flip injection because a more negative bias application is necessary to form the excess electrons in the QDs. Further p-doping of 15 holes/QD pushes this negative CPD bias condition toward a more negative bias side, such as approximately −2.2 V. Some information is also provided. The bias range indicating negative CPDs becomes wider with p-doping than without doping. A strong negative CPD also appears beyond −2 V in the 5 holes/QD sample; however, the PL intensity is rather weak in this bias range, and therefore, this bias effect can be negligible in terms of the device performance. The inhomogeneous doping concentration in the QD ensemble is likely to cause the broadening of the bias condition with negative CPDs. Precise control of the hole concentration and consequent optimization will be an important next step in expanding this research theme. The present doping of the capping layer is known to work well for self-assembled QDs, but the hole concentration uniformity also needs to be improved. This doping uniformity can be improved by improving dot uniformity, such as dot size and density, which can be achieved by increasing the dot density in addition to optimizing the growth conditions. Potential calculations as a function of the electric field, as shown in Figure 1b, suggest that other remote p-doping can be applied to the upper AlGaAs barrier adjacent to the GaAs capping layer. This distant p-doping from the surrounding layer will be efficient in improving the crystal quality of the capping layer and thus the QD performances.

Next, the excitation power dependences of both positive and negative CPD values are shown in Figure 4.

https://dx.doi.org/10.1021/acsomega.1c00377
ACS Omega 2021, 6, 8561−8569

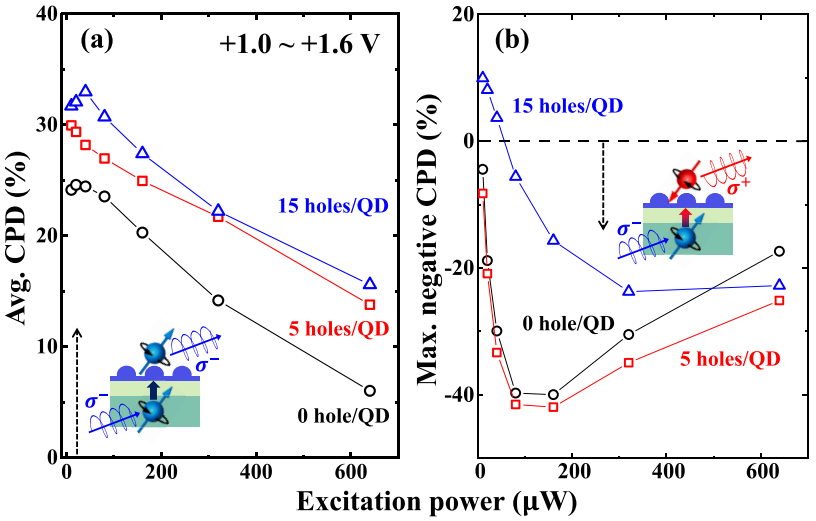

Figure 4. (a) Averaged CPD value in a bias range of +1.0 to +1.6 V, indicating the degree of parallel spin polarization, and (b) maximum negative CPD value, indicating the degree of antiparallel polarization, at the optimal bias voltage, as a function of excitation power at the QD-GS, for the 0 hole/QD (black open circles), 5 holes/QD (red open squares), and 15 holes/QD (blue open triangle) samples. The parallel spin injection and the spin-flip injection processes are schematically shown as insets in (a) and (b), respectively.

As can be seen, the 5 holes/QD doping condition can provide high values of negative CPD (b: electric-field-induced spin-flip injection) as well as positive CPD (a: parallel spin injection). Higher positive CPD values at the GS with higher PL intensities by p-doping have been reported.[30,31] Increasing oscillator strength and suppressing electron spin relaxation by p-doping are responsible for the improved normal parallel electron spin injection. Bir−Aronov−Pikus (BAP) spin relaxation is well known to be dominant in QDs, where a hole-exchange field acts on the electron spin.[1,40] Excess holes by p-doping can randomize the hole field, and the BAP spin relaxation can be suppressed.[31] Both positive and negative CPD values decreased with increasing excitation power for all samples. The positive CPD reduction can be induced by a spin-state filling effect at the QD-ESs after spin injection from the QW.[35,36] Parallel spin injection from the QW into the QD-ESs can be blocked by the Pauli exclusion principle with strong excitation powers. In contrast, minority antiparallel spins can be continuously injected during spin blocking and can reduce the spin polarization *P*. However, it is important to stress that the electric-field effect of spin-flip injection, as well as normal parallel spin injection, can be optimized by the p-doping concentration, such as with the 5 holes/QD condition. The PL intensity can also be strongly enhanced by this p-doping. Therefore, remote p-doping in this characteristic coupled QW/QD structure is promising for the development of semiconductor-based electric-field-effect optical spin device performance.

The spin dynamics in the QDs after the spin injection from the QW were detected to clarify the mechanism of p-doping effects on the electric-field spin reversal. The circularly polarized time-resolved PL and the resultant CPD are shown for the QD-ES as well as the GS in Figure 5, where the bias conditions are selected to show marked negative CPD properties at the GS. Data variability is noticeable at the ES of the 15 holes/QD sample (bottom panel in Figure 5a). This is due to the weaker PL intensity of the ES under bias conditions that show the highest negative CPD value in this sample compared to other samples. In this 15 holes/QD sample, the hole concentration is not particularly high in the

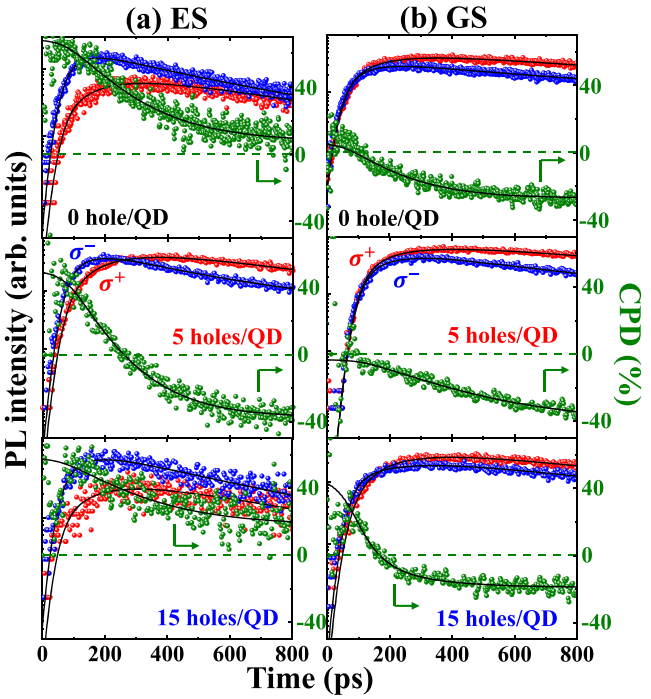

Figure 5. Time dependences of circularly polarized PL intensity (red closed circles: σ^+ of antiparallel polarization to the initial one in the QW; blue closed circles: σ^- of parallel polarization) and the corresponding CPD values (green closed circle) at (a) the 1st ES and (b) the GS with an excitation power of 160 μW, for the 0 hole/QD (top panel), 5 holes/QD (middle panel), and 15 holes/QD (bottom panel) samples, respectively. The applied voltages are selected for the cases of the highest negative CPD values, such as 0, −0.45, and −2.2 V, for the 0, 5, and 15 holes/QD samples. Rate-equation calculations, taking an asymmetric spin-flip process in addition to the usual spin relaxation and a system time response are shown by a black narrow line.

ES of QD after initial recombination by a large number of injected electrons due to the strong potential modification, as shown in Figure 1b. The doped holes at the ES can also escape from the QD to the QW side, while those at the GS tend to be

https://dx.doi.org/10.1021/acsomega.1c00377
ACS Omega 2021, 6, 8561−8569

more confined in the QD, originating from this strong negative-bias-induced valence-band bending.

The CPD decaying properties at ESs indicate the spin-flip dynamics via electron−hole scattering in addition to the usual spin-relaxation-induced CPD decaying with the time constants around 0.5 ns.[38,39] The 5 holes/QD sample shows the most significant spin-flip dynamics at the ES, where parallel spins flip rapidly after the spin injection from the QW, and then start to show the negative CPD at 250 ps. The appearance of negative CPD directly shows that the spin-flipped electrons become dominant even at the ES. This rapid spin-flip can be induced by hole doping, which promotes efficient electron−hole scattering. These time-dependent PL decay curves and the resultant CPD changes both in the ES and GS were well fitted by rate equations taking into account an asymmetric spin-flip process at the ES,[41] which are indicated by black solid lines in Figure 5. Time−response curves of a measurement system are also included.

The deduced asymmetric spin-flip time τ_{sf} as a function of excitation power at the ES is plotted for all samples in Figure 6.

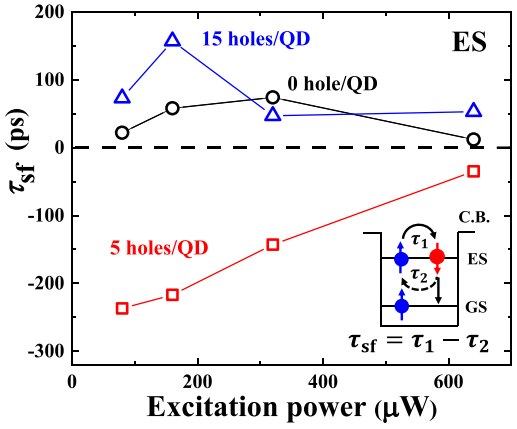

Figure 6. Asymmetric spin-flip time constant τ_{sf}, derived from the rate-equation fitting for the circularly polarized time-resolved PL at the ES, as a function of excitation power for the samples with 0 hole/QD (black open circles), 5 holes/QD (red open squares), or 15 holes/QD (blue open triangles). The inset shows schematically the asymmetric spin-flip process with a time constant of $\tau_{sf} = \tau_1 - \tau_2$. $\tau_{sf} = 0$ corresponds to the symmetric spin-flip dynamics with usual spin relaxation times. The applied voltages are selected for the cases of the highest negative CPD values, such as 0, −0.45, and −2.2 V, for the 0, 5, and 15 holes/QD samples.

This asymmetric spin-flip can be attributed to a combination of the spin-flip process at the ES and the subsequent energy relaxation from the ES to GS, which is schematically illustrated as an inset in Figure 6.[37] The spin-flip itself can originate from the spin scattering in addition to the usual symmetric spin relaxation. The asymmetric flip property can be induced by filling a spin-dependent state at the GS that is energetically below the ES, where the presence of residual electrons can prevent this energy relaxation and therefore induce the asymmetric spin-flip at the ES. The spin scattering events also depend on the presence of spin-polarized holes within the QD. A negative τ_{sf} value means the asymmetric spin-flip from the parallel spin into the reversed one, which can be induced by the state filling at the GS with the residual parallel spin. It should be noted that the usual spin relaxation with a symmetric time constant, which promotes time-dependent randomization of the spin direction, takes place in all samples independent of the above asymmetric spin-flip process. This constant spin relaxation time is included in the above rate-equation analysis. As can be seen, the 5 holes/QD sample only shows a significant trend of negative τ_{sf} values at the ES. Therefore, this 5 holes/QD sample demonstrates an enhanced efficient spin reversal at the ES as a result of suitable p-doping. This enhanced spin reversal is suppressed at high excitation powers, resulting from the state filling at the GS. In contrast, the other samples including the highest doping sample of 15 holes/QD show nearly zero or slightly positive τ_{sf} values at the ES, which indicates that the asymmetric spin-flip process is not active. Therefore, the negative CPD values in the PL in these nondoped and 15 holes/QD samples are realized mainly by the usual, thus symmetric, spin relaxation at the ES.

These spin dynamics directly show the electron spin-flip process during spin injection in this characteristic coupled QD/QW nanosystem. In the undoped reference sample, this spin-flip process can be realized by field applications with a markedly narrow bias range as shown in Figure 3b, in which a residual electron with the parallel spin direction exists at the QD-GS without a hole before the spin injection, as schematically shown in Figure 7a.

An electron−hole pair with conserved spin states is then injected from the QW, and this electron spin can be scattered with the hole spin at the ES. A spin-flipped electron only can relax to the GS and subsequently recombine with the hole, emitting negatively polarized PL. Moreover, one can guess that the above situation with an efficient electron−hole pair injection, as well as the presence of a residual electron, is not equally achieved among QDs in that narrow bias range in this 0 hole/QD sample. The hole tunneling rate can be significantly affected by the shape and size distributions of the QD ensemble because of the heavier effective mass than that of electrons. As a result, the PL intensity with the negative CPD is markedly low because the number of QDs emitting spin-polarized PL is rather limited.

However, the optimum remote p-doping into the QD ensemble can significantly improve this problem, as shown in Figure 7b. More negative bias conditions can realize the same situation as discussed above for the undoped QDs, where a residual electron with the parallel spin state exists at the GS after recombination with doped holes with the same parallel spin. Then, further parallel spin-polarized electrons can be injected from the QW, and the abovementioned spin scattering can take place at the ES, resulting in a negative CPD property at the GS after relaxation. It is important to note that this more negative bias condition for the 5 holes/QD sample gives a higher electron spin tunneling probability in this coupled QD/QW system, as shown in Figure 1b. Therefore, many QDs contain residual electrons, and also the electron−hole pairs can be efficiently injected for many QDs with residual electrons. On the other hand, under this bias condition, holes are less likely to be injected from the well, also as viewed from the potential in Figure 1b. Doped holes with a spin parallel to the injected electron spin can compensate for the absence of hole injection so that the parallel electron−hole spins recombine and disappear by the initial spin-conserving electron injection. Therefore, doped holes with an opposite spin to the residual electron spin can remain in the GS and even in the ES in the QDs. Electron spins injected into the ES can relax to the GS after efficient spin-flip scattering. Here, as depicted in Figure 7b, if electron spins are rapidly injected one after another, the

https://dx.doi.org/10.1021/acsomega.1c00377
ACS Omega 2021, 6, 8561−8569

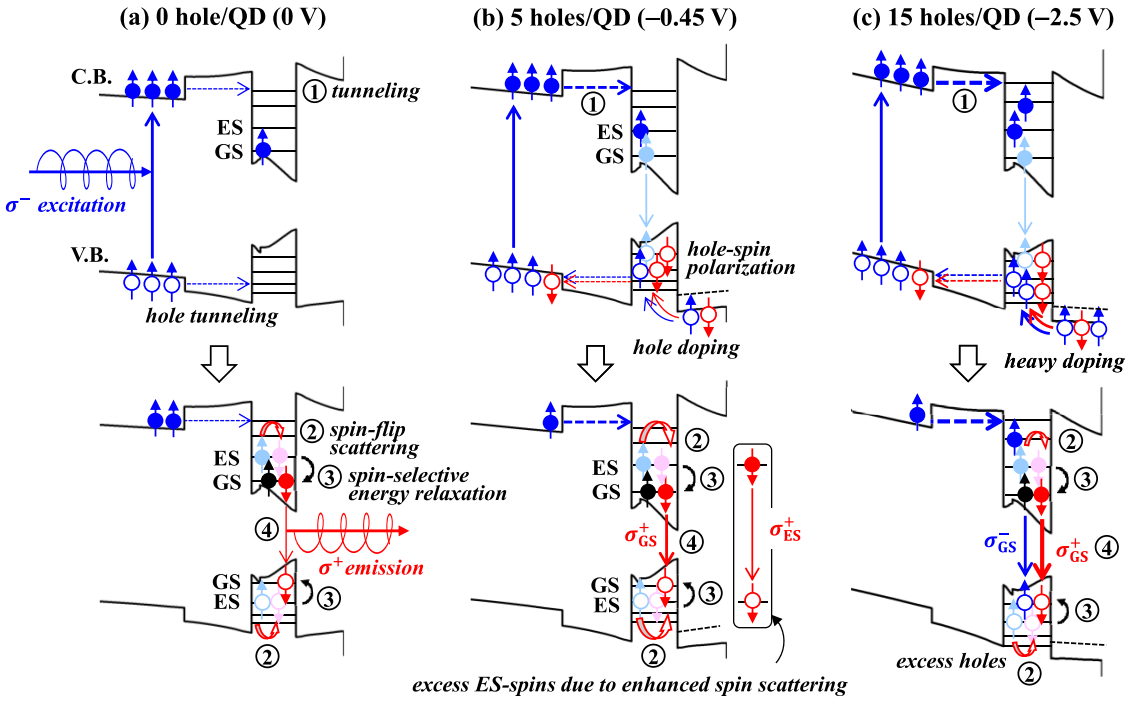

Figure 7. Schematic illustrations of the electric-field-induced reversed-spin injection process from the QW into the QD-GS and the resultant circularly polarized emissions, including the spin-flip process at the ES during the injection, for samples with optimum biases such as (a) 0 hole/QD at 0 V, (b) 5 holes/QD at −0.45 V, and (c) 15 holes/QD at −2.5 V. A blue closed spin image in the conduction band shows optically generated initial spin-polarized electrons in the QW, which can be injected into the QD via tunneling. A black closed spin image indicates a residual electron spin in the QD, which can be formed by excess electron spin injection owing to the electric-field-induced coupled potential modification. A red closed spin image indicates spin-flipped electrons resulting from the electron−hole scattering at ESs.

excited hole spins are inverted again and cannot be relaxed to the GS. Meanwhile, the electron spin relaxes to the GS after the spin-flip and recombines with the hole spin at the GS emitting negative CPD. That is, spin-flip scattering occurs efficiently due to the combination of electric-field-induced enhanced electron tunneling probability with appropriate doping. Furthermore, hole spins can be trapped by many dots by this p-doping, which increases the number of optically active dots. Therefore, spin scattering can occur efficiently at the ESs in many QDs, and as a result, electron spins can be flipped and the number of dot-emitting PL with negative CPDs increases. In other words, one can conclude that this 5 holes/QD condition is highly efficient for improving this unique electric-field spin-functional optical device.

The higher doping sample of 15 holes/QD shows a shift in the operating bias for the negative CPD toward the more negative bias side, as shown in Figure 7c. More electrons need to be injected to compensate for more holes in the QDs. Therefore, a higher negative bias needs to be applied to cause this negative CPD phenomenon. However, when many electron spins are injected into the QD-ESs, the spin polarization degree of the injected electrons decreases owing to the state-filling effect, as discussed above, for the case where the positive CPD decreases with increasing excitation power. This excess electron injection after forming a residual electron at each QD can also prevent the efficient spin-flip at the ES; for instance, co-scattering can maintain the original electron spin state. The BAP electron spin relaxation mechanism is known to show that the spin-relaxation time decreases with increasing hole concentration by increasing the exchange-field strength of the hole against an electron spin. Therefore, it is suggested that this heavier p-doping condition can offer mainly two holes at the ES of each QD since many excess holes can escape from the QD into the QW side depending on this strong negative bias, as shown in Figure 1b.

4. CONCLUSIONS

We have studied the effects of p-doping on the electric-field control of electron and photon spin polarity in a coupled InGaAs QD/QW nanosystem. Remote p-doping in the QDs tunnel-coupled with the QW significantly increased the circularly polarized PL intensity from the QD-GSs after electron spin injection from the QW as a spin reservoir. The spin polarity during this spin injection can be controlled by the direction of the electric field and the strength driving this electron injection, where the spin reversal can be induced by excess electron spin injection into the QDs via spin scattering at the QD-ESs. We found that the maximum degrees of both spin polarization with parallel and antiparallel spin polarities can be optimized by the hole concentration. Therefore, p-doping is highly effective for the electric-field-effect spin switching with an enhanced number of spins. This optimized p-doping exhibited the fastest spin reversal at the QD-ESs, resulting in an efficient electric-field-driven antiparallel spin injection for the GS with a moderate electric-field application. Further excess hole doping prevented this efficient spin reversal due to multiple electron−hole spin scatterings, as well as an electron spin state filling effect during the spin injection from the QW into the QDs.

AUTHOR INFORMATION

Corresponding Author

Akihiro Murayama − *Faculty of Information Science and Technology, Hokkaido University, Sapporo 060-0814,*

https://dx.doi.org/10.1021/acsomega.1c00377
ACS Omega 2021, 6, 8561−8569

Japan; orcid.org/0000-0001-5140-4070;
Email: murayama@ist.hokudai.ac.jp

Authors

Soyoung Park − *Faculty of Information Science and Technology, Hokkaido University, Sapporo 060-0814, Japan*
Hang Chen − *Faculty of Information Science and Technology, Hokkaido University, Sapporo 060-0814, Japan*
Satoshi Hiura − *Faculty of Information Science and Technology, Hokkaido University, Sapporo 060-0814, Japan*; orcid.org/0000-0002-0710-2777
Junichi Takayama − *Faculty of Information Science and Technology, Hokkaido University, Sapporo 060-0814, Japan*; orcid.org/0000-0001-9800-5069
Kazuhisa Sueoka − *Faculty of Information Science and Technology, Hokkaido University, Sapporo 060-0814, Japan*

Complete contact information is available at:
https://pubs.acs.org/10.1021/acsomega.1c00377

Notes

The authors declare no competing financial interest.

■ ACKNOWLEDGMENTS

This work was supported by the Japan Society for the Promotion of Science (JSPS), Grant Numbers 16H06359, 19K15380, and 19H05507.

■ REFERENCES

(1) Dyakonov, M. I.; Perel, V. I. Theory of Optical Spin Orientation of Electrons and Nuclei in Semiconductors. In *Optical Orientation*, Meier, F.; Zakharchenya, B. P., Eds.; North-Holland: Amsterdam, 1984; pp 11−71.
(2) Dyakonov, M. I. Basics of Semiconductor and Spin Physics. In *Spin Physics in Semiconductors*, Dyakonov, M. I., Ed.; Springer, 2008; pp 1−28.
(3) Baibach, M. N.; Broto, J. M.; Fert, A.; Nguyen, F.; Van Dau Petroff, F.; Etienne, P.; Creuset, G.; Friederich, A.; Chazelas, J. Giant Magnetoresistance of (001)Fe/(001)Cr Magnetic Superlattices. *Phys. Rev. Lett.* **1988**, *62*, 2472−7475.
(4) Miyazaki, T.; Tezuka, N. Giant magnetic tunneling effect in Fe/Al_2O_3/Fe junction. *J. Magn. Magn. Mater.* **1995**, *139*, L231−L234.
(5) Wolf, S. A.; Awschalom, D. D.; Buhrman, R. A.; Daughton, J. M.; von Molnar, S.; Roukes, M. L.; Chtchelkanova, A. Y.; Treger, D. M. Spintronics: A Spin-Based Electronics Vision for the Future. *Science* **2001**, *294*, 1488−1495.
(6) Yuasa, S.; Nagahama, T.; Fukushima, A.; Suzuki, Y.; Ando, K. Giant room-temperature magnetoresistance in single-crystal Fe/MgO/Fe magnetic tunnel junction. *Nat. Mater.* **2004**, *3*, 868−871.
(7) Arakawa, Y.; Sakaki, H. Multidimensional quantum well laser and temperature dependence of its threshold current. *Appl. Phys. Lett.* **1982**, *40*, 939−941.
(8) Arakawa, Y.; Yariv, A. Quantum well lasers-Gain, spectra, dynamics. *IEEE J. Quantum Electron.* **1986**, *22*, 1887−899.
(9) Mukai, K.; Nakata, Y.; Shoji, H.; Sugawara, M.; Ohtsubo, K.; Yokoyama, N.; Ishikawa, H. Lasing with low threshold current and high output power from columnar-shaped InAs/GaAs quantum dots. *Electron. Lett.* **1998**, *34*, No. 1588.
(10) Amano, T.; Sugaya, T.; Komori, K. Characteristics of 1.3μm quantum-dot lasers with high-density and high-uniformity quantum dots. *Appl. Phys. Lett.* **2006**, *89*, No. 171122.
(11) Akahane, K.; Yamamoto, N.; Tsuchiya, M. Highly stacked quantum-dot laser fabricated using a strain compensation technique. *Appl. Phys. Lett.* **2008**, *93*, No. 041121.
(12) Higo, A.; Kiba, T.; Tamura, Y.; Thomas, C.; Takayama, J.; Wang, Y.; Sodabanlu, H.; Sugiyama, M.; Nakano, Y.; Yamashita, I.; Murayama, A.; Samukawa, S. Light-Emitting Devices Based on Top-down Fabricated GaAs Quantum Nanodisks. *Sci. Rep.* **2015**, *5*, No. 9371.
(13) Sugawara, M.; Usami, M. Handling the heat. *Nat. Photon* **2009**, *3*, 30−31.
(14) Chen, S.; Li, W.; Wu, J.; Jiang, Q.; Tang, M.; Shutts, S.; Elliott, S. N.; Sobiesierski, A.; Seeds, A. J.; Ross, I.; Smowton, P. M.; Liu, H. Electrically pumped continuous-wave III−V quantum dot lasers on silicon. *Nat. Photon* **2016**, *10*, 307−311.
(15) Khaetskii, A. V.; Nazarov, Y. V. Spin relaxation in semiconductor quantum dots. *Phys. Rev. B* **2000**, *61*, 12639−12642.
(16) Paillard, M.; Marie, X.; Renucci, P.; Amand, T.; Jbeli, A.; Gérard, J. M. Spin Relaxation Quenching in Semiconductor Quantum Dots. *Phys. Rev. Lett.* **2001**, *86*, 1634−1637.
(17) Borri, P.; Langbein, W.; Schneider, S.; Woggon, U.; Sellin, R. L.; Ouyang, D.; Bimberg, D. Ultralong Dephasing Time in InGaAs Quantum Dots. *Phys. Rev. Lett.* **2001**, *87*, No. 157401.
(18) Elzerman, J. M.; Hanson, R.; Willems van Beveren, L. H.; Witkamp, B.; Vandersypen, L. M. K.; Kouwenhoven, L. P. Single-shot read-out of an individual electron spin in a quantum dot. *Nature* **2004**, *430*, 431−435.
(19) Kroutvar, M.; Ducommun, Y.; Heiss, D.; Bichler, M.; Schuh, D.; Abstreiter, G.; Finley, J. J. Optically programmable electron spin memory using semiconductor quantum dots. *Nature* **2004**, *432*, 81−84.
(20) Chye, Y.; White, M. E.; Johnston-Halperin, E.; Gerardot, B. D.; Awschalom, D. D.; Petroff, P. M. Spin injection from (Ga,Mn)As into InAs quantum dots. *Phys. Rev. B* **2002**, *66*, No. 201301(R).
(21) Li, C. H.; Kioseoglou, G.; van't Erve, O. M. J.; Ware, M. E.; Gammon, D.; Stroud, R. M.; Jonker, B. T.; Mallory, R.; Yasar, M.; Petrou, A. Electrical spin pumping of quantum dots at room temperature. *Appl. Phys. Lett.* **2005**, *86*, No. 132503.
(22) Lombez, L.; Renucci, P.; Braun, P. F.; Carrère, H.; Marie, X.; Amand, T.; Urbaszek, B.; Gauffier, J. L.; Gallo, P.; Camps, T.; Arnoult, A.; Fontaine, C.; Deranlot, C.; Mattana, R.; Jaffrès, H.; George, J.-M.; Binh, P. H. Electrical spin injection into p-doped quantum dots through a tunnel barrier. *Appl. Phys. Lett* **2007**, *90*, No. 081111.
(23) Basu, D.; Saha, D.; Wu, C. C.; Holub, M.; Mi, Z.; Bhattacharya, P. Electrically injected InAs/GaAs quantum dot spin laser operating at 200K. *Appl. Phys. Lett.* **2008**, *92*, No. 091119.
(24) Chen, H.; Hiura, S.; Takayama, J.; Park, S.; Sueoka, K.; Murayama, A. Electric field control of spin polarity in spin injection into InGaAs quantum dots from a tunnel-coupled quantum well. *Appl. Phys. Lett.* **2019**, *114*, No. 133101.
(25) Pal, B.; Verbin, S. Yu.; Ignatiev, I. V.; Ikezawa, M.; Masumoto, Y. Nuclear-spin effects in singly negatively charged InP quantum dots. *Phys. Rev. B* **2007**, *75*, No. 125322.
(26) Puttisong, Y.; Haung, Y.; Buyanova, I.; Yang, X. J.; Subagyo, A.; Sueoka, K.; Murayama, A.; Chen, W. M. Anomalous spectral dependence of optical polarization and its impact on spin detection in InGaAs/GaAs quantum dots. *Appl. Phys. Lett.* **2014**, *105*, No. 132106.
(27) Kalevich, V. K.; Merkulov, I. A.; Shiryaev, A. Yu.; Kavokin, K. V.; Ikezawa, M.; Okuno, T.; Brunkov, P. N.; Zhukov, A. E.; Ustinov, V. M.; Masumoto, Y. Optical spin polarization and exchange interaction in doubly charged InAs self-assembled quantum dots. *Phys. Rev. B* **2005**, *72*, No. 045325.
(28) Laurent, S.; Senes, M.; Krebs, O.; Kalevich, V. K.; Urbaszek, B.; Marie, X.; Amand, T.; Voisin, P. Negative circular polarization as a general property of n-doped self-assembled InAs/GaAs quantum dots under nonresonant optical excitation. *Phys. Rev. B* **2006**, *73*, No. 235302.
(29) Shabaev, A.; Stinaff, E. A.; Bracker, A. S.; Gammon, D.; Efros, A. L.; Korenev, V. L.; Merkulovet, I. Optical pumping and negative luminescence polarization in charged GaAs quantum dots. *Phys. Rev. B* **2009**, *79*, No. 035322.
(30) Taylor, M. W.; Harbord, E.; Spencer, P.; Clarke, E.; Slavcheva, G.; Murray, R. *Appl. Phys. Lett.* **2010**, *97*, No. 171907.

(31) Taylor, M. W.; Spencer, P.; Murray, R. Optical spin-filtering effect in charged InAs/GaAs quantum dots. *Appl. Phys. Lett.* **2015**, *106*, No. 122404.
(32) Chen, H.; Hiura, S.; Takayama, J.; Park, S.; Sueoka, K.; Murayama, A. Enhanced hetero-dimensional electron-spin injection in a resonantly tunnel-coupled InGaAs quantum dot−well nanosystem. *Appl. Phys. Express* **2020**, *13*, No. 015003.
(33) Brataas, A.; Kent, A. D.; Ohno, H. Current-induced torques in magnetic materials. *Nat. Mater.* **2012**, *11*, 372−381.
(34) Liu, L.; Pai, C. F.; Li, Y.; Tseng, H. W.; Ralph, D. C.; Buhrman, R. A. Spin-Torque Switching with the Giant Spin Hall Effect of Tantalum. *Science* **2012**, *336*, 555−558.
(35) Cai, K.; Yang, M.; Ju, H.; Wang, S.; Ji, Y.; Li, B.; Edmonds, K. W.; Sheng, Y.; Zhang, B.; Zhang, N.; Liu, S.; Zheng, H.; Wang, K. Electric field control of deterministic current-induced magnetization switching in a hybrid ferromagnetic/ferroelectric structure. *Nat. Mater.* **2017**, *16*, 712−716.
(36) Cao, Y.; Sheng, Y.; Edmonds, K. W.; Ji, Y.; Zheng, H.; Wang, K. Deterministic Magnetization Switching Using Lateral Spin−Orbit Torque. *Adv. Mater.* **2020**, *32*, No. 1907929.
(37) Birner, S.; Zibold, T.; Andlauer, T.; Kubis, T.; Sabathil, M.; Trellakis, A.; Vogl, P. nextnano: General Purpose 3-D Simulations. *IEEE Trans. Electron. Devices* **2007**, *54*, 2137−2142.
(38) Kiba, T.; Yang, X.; Yamamura, T.; Kuno, Y.; Subagyo, A.; Sueoka, K.; Murayama, A. Temperature dependence of the dynamics of optical spin injection in self-assembled InGaAs quantum dots. *Appl. Phys. Lett.* **2013**, *103*, No. 082405.
(39) Yamamura, T.; Kiba, T.; Yang, X.; Takayama, J.; Subagyo, A.; Sueoka, K.; Murayama, A. Growth-temperature dependence of optical spin-injection dynamics in self-assembled InGaAs quantum dots. *J. Appl. Phys.* **2014**, *116*, No. 094309.
(40) Bir, G. L.; Aronov, A. G.; Pikus, G. E. Spin relaxation of electrons due to scattering by holes. *Zh. Eksp. Teor. Fiz.* **1975**, *69*, 1382−1397.
(41) Hiura, S.; Hatakeyama, S.; Takayama, J.; Murayama, A. Asymmetric spin relaxation induced by residual electron spin in semiconductor quantum-dot-superlattice hybrid nanosystem. *Appl. Phys. Lett.* **2020**, *116*, No. 262407.

https://dx.doi.org/10.1021/acsomega.1c00377
ACS Omega 2021, 6, 8561−8569